

Corrosion of Mild Steel Under Anaerobic Biofilm[☆]

W. Lee and W.G. Characklis^{*}

ABSTRACT

Corrosion of mild steel under completely anaerobic conditions in the presence of a mixed population biofilm, including sulfate-reducing bacteria (SRB), has been studied in a continuous flow system. The closed channel flow reactor was continuously fed with low concentration substrate at different dilution rates that influenced biofilm accumulation. No direct correlation was observed between corrosion and SRB activity in the absence of ferrous iron. Furthermore, corrosion of mild steel in the SRB environment was determined by the nature of the metal and environmental conditions such as dissolved iron concentration. When formation of an iron sulfide film on mild steel was prevented before the biofilm accumulated, the metal surface retained its scratch lines after a 21-day experiment (SRB at $2.6 \times 10^9/cm^2$). However, when the iron sulfide film was formed before the accumulation of biofilm, visible localized corrosion appeared after 14 days and increased up to 21 days. Intergranular and pitting attack was found in the localized corrosion area. Inclusions (Al, Mn, and Fe) and grain boundary triple points were also found in the localized corrosion area. At high iron concentration (approximately 60 mg/L in the bulk water), all biogenic sulfide was precipitated and corrosion had significantly enhanced. Intergranular attack was found over the entire metal surface.

KEY WORDS: carbon steel, depolarization, microbial corrosion, pitting potential, polarization

INTRODUCTION

Under abiotic conditions, there is very little, if any, corrosion of steel in the absence of oxygen under neutral or alkaline conditions because the cathode becomes polarized by the build-up of a layer of atomic hydrogen.¹ However, anaerobic corrosion may occur in the presence of sulfide due to cathodic depolarization ($2 H_2S + 2 e^- \rightarrow 2 HS^- + H_2$). The attack was not only by dissolved sulfide but also by iron sulfide.² Iron sulfide causes cathodic depolarization by decreasing the hydrogen overpotential, but the site of the hydrogen reduction reaction is unknown.

Biotic production of sulfide may lead to corrosion of mild steel in anaerobic environments. For example, chemostat (planktonic cells) investigations indicate that microbial sulfide production leads to cathodic depolarization primarily due to the iron sulfide reaction.³ Booth et al.^{4,5} reported that no correlation exists between hydrogenase activity and corrosion rate when experiments were undertaken in semicontinuous and continuous culture in high- or low-ferrous medium. The corrosion rate was controlled by the stability of an iron sulfide film on the steel surface. In field investigations, Starkey reported that only slight corrosion of a completely buried steel pipe was

^{*} Submitted for publication September 1991; in revised form, September 1992.

^{*} Center for Interfacial Microbial Process Engineer, Montana State University, Bozeman, MT 59717.

detected in anaerobic mud supporting an active community of sulfate-reducing bacteria (SRB).⁶

V.W. Kühr and van der Vlugt⁷ proposed the cathodic depolarization theory for microbial (SRB) corrosion-based on batch (closed) reactor investigations. They suggested that hydrogenase catalyzed the hydrogen reduction reaction on the iron surface. King and Miller⁸ supported the hydrogenase theory but proposed that cathodic depolarization occurred on the iron sulfide instead of the iron surface. Costello⁹ reports that *desulfovibrio desulfuricans* in a batch reactor produces H₂S, which directly depolarizes the cathode. In summary, there is evidence for cathodic depolarization as an important mechanism in the anaerobic corrosion of iron and mild steel. However, the exact mechanism, including the role of hydrogenase, is not definitively understood.

Most microbial corrosion in nature and in technological systems occurs in association with microbial aggregates or biofilms. Hamilton¹⁰ has developed a qualitative biofilm model of anaerobic microbial corrosion where the growth of biofilm SRB requires that the appropriate physicochemical conditions be supplied by other facultative and anaerobic organisms within the biofilm. To address the anaerobic microbial corrosion problems in natural environments, the activities and behavior of biofilm or sessile SRB, not planktonic SRB, must be considered.

There is very little quantitative information available related to the rate and extent of microbial sulfide production in biofilms. Nielsen¹¹ reports kinetic data from a continuous flow SRB biofilm reactor, which indicates that sulfate diffusion in the biofilm is rate-limiting for SRB biofilm activity.

The relation between SRB activity and the corrosion rate of mild steel is still not well established despite decades of research. Progress in microbial corrosion research has been limited by at least two factors: (1) lack of experimental methods that simulate biofilm processes in continuous systems and (2) lack of analytical techniques that can be used in a biofilm system while still providing adequate characterization of the corroding metal surface.

This investigation was conducted with a mixed population biofilm containing SRB in a continuous flow closed channel reactor that simulates some of the important characteristics of relevant industrial systems. The objectives of the study were to determine (1) the effect of substrate loading rate on the corrosion of mild steel in the absence of ferrous iron, (2) the correlation of SRB activity with the cathodic depolarization reaction, (3) the effect of the iron sulfide film on the corrosion of mild steel in the presence of biofilm, and (4) the effect of suspended iron sulfide on the corrosion of mild steel in the presence of biofilm. Substrate loading rate is the product of the dilution

rate and influent lactate concentration divided by the surface area to volume ratio.

EXPERIMENTAL

Experimental Reactor

All experiments were conducted in a continuous closed channel flow reactor with dimensions 1.00 by 0.15 by 0.30 m, containing a working volume of 4.5 L with a surface area of 0.35 m² (Figure 1). The reactor had a recirculation loop to provide sufficient mixing and a flow velocity of approximately 0.3 m/s. The experimental system was purged with nitrogen to minimize air permeation. Before entering the reactor, the purge gas was passed through hot copper filings to remove traces of oxygen. The reactor contained 24 corrosion coupons that were connected to a potentiostat. The dilution rate (influent flow rate divided by working volume) was the inverse of residence time and was varied without influencing flow velocity in the channel.

Media and Biofilm Growth Conditions

Bacteria were grown in 1/10 strength artificial seawater, 200 mg/L lactic acid, 50 mg/L yeast extract, 50 mg/L NH₄Cl, and 5 mg/L Na₂HPO₄. Ferrous iron was absent in the media except in the last experiment. The pH was controlled at 8 with 0.1 N NaOH and 0.1 N HCl; they were both flushed with nitrogen and reduced by adding 0.013% Na₂SO₃. Temperature was controlled at 30°C by a heat exchanger and cooler. *Desulfovibrio desulfuricans* was inoculated into the open-channel flow reactor, which, for the first week, was operated as a batch reactor until surface colonization occurred. Thereafter, substrate was continuously fed to the reactor. The experiment was not conducted aseptically in order to simulate natural marine environments in which the SRB grow.

Coupons

Disks of AISI 1018 (UNS⁽¹⁾ G10180) mild steel, 15.9 mm in diameter, were cast in acrylic resin to avoid the risk of crevice corrosion. The coupons were polished with a series of grit papers (120, 200, 320, 400, 600) followed by ultrasonic cleaning in 100% alcohol for one minute and dried in air at room temperature.

Corrosion Measurements

Corrosion potential, cathodic polarization, pitting potential, alternating current (AC) impedance, and weight loss were measured in the open channel flow

⁽¹⁾ UNS numbers are listed in *Metals and Alloys in the Unified Numbering System*, published by the Society of Automotive Engineers (SAE) and cosponsored by ASTM.

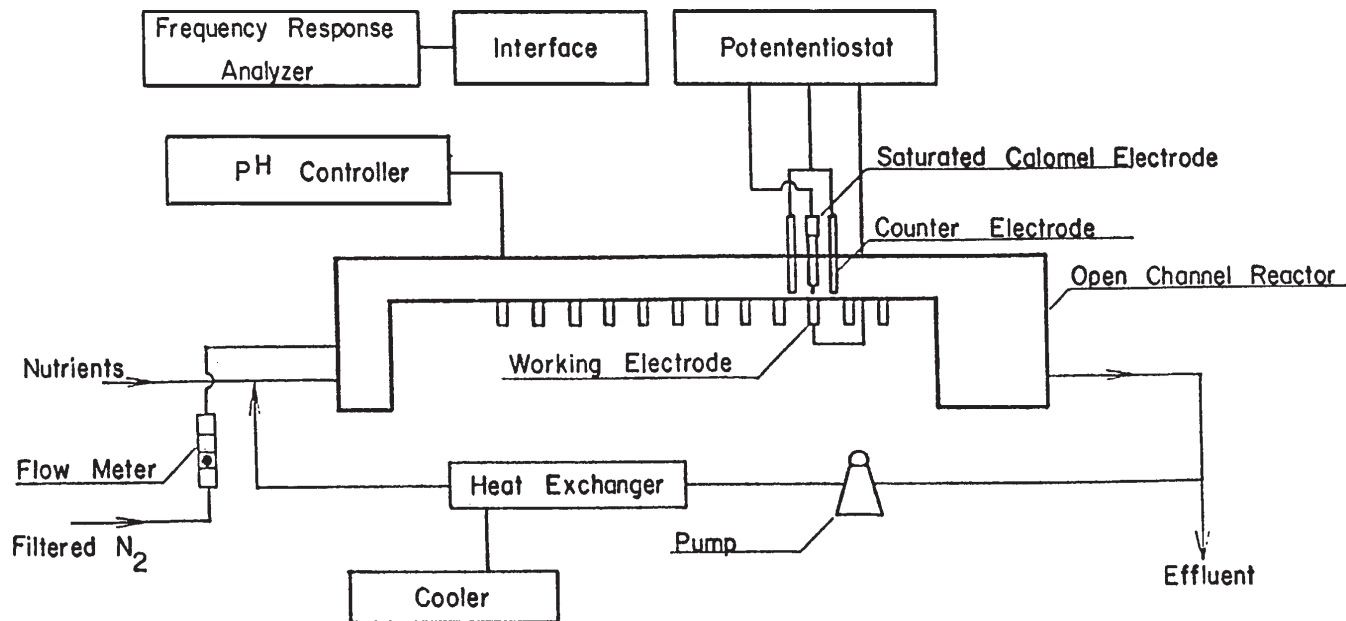


FIGURE 1. Continuous open channel flow reactor with dimensions 1.00 by 0.15 by 0.30 m and with a working volume of 4.5 L.

reactor periodically for up to 21 days. Direct current (DC) measurements were made using a potentiostat/galvanostat and AC measurements were made using a frequency response analyzer through an electrical interface.

The potential of the working electrode was measured against a saturated calomel electrode (SCE). Two graphite rods were used as counter electrodes. Cathodic polarization measurements were performed from E_{corr} to 400 mV in the cathodic direction at a scan rate 0.2 mV/s. Pitting potential measurements were performed beginning at -800 mV in the anodic direction with the same scan rate as cathodic polarization. AC impedance measurements were made using a sine wave voltage with an amplitude of 7.5 mV at frequencies between 2 mHz and 10 kHz. Ten frequencies were examined per decade. At the end of each experiment, coupons were removed from the reactor and cleaned in an ultrasonic bath with an inhibited acid solution for 30 s prior to the weight loss measurement.

Water Chemistry

Desulfovibrio desulfuricans uses lactate as a carbon and energy source and oxidizes it to acetate coupled with the reduction of sulfate to sulfide. As a consequence, the chemical analysis of the reactor fluid included lactate, acetate, sulfate, total dissolved sulfide, and redox potential. Samples were taken from

both influent and effluent to complete material balances.

Lactate was determined by an enzymatic method. Acetate was measured with a gas chromatograph. Sulfate concentration was determined using the barium chloride turbidimetric method.¹² Total dissolved sulfide was determined by adding zinc acetate to precipitate sulfide followed by the methylene blue method.¹³ The redox potential was determined by measuring the potential of a platinum electrode using the potentiostat/galvanostat against a saturated calomel electrode.

Biological Analysis

SRB numbers in the biofilm were determined by the five tube multiple dilution most probable number (MPN) method using Postgate B broth. A metal coupon covered with biofilm was removed from the reactor and transferred to an anaerobic tent in which the biofilm was removed by brushing into 30 mL of sterile 1/10 artificial seawater and homogenized to disperse the biofilm. A dilution series to 10^{-10} was prepared from 1 mL of the suspended biofilm solutions. SRB numbers in the bulk water were determined by the same MPN method for a 1 mL sample. Numbers of general anaerobic bacteria (GAB) both in the biofilm and bulk water were determined by the same procedure as that for SRB except that fluid thioglycollate medium was used.

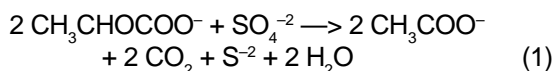
Surface Analysis of Biofilm and Corrosion Products

A biofilm sample was transferred anaerobically to the anaerobic tent and fixed for 8 h in 2% glutaraldehyde diluted with filter-sterilized artificial seawater. Then, the sample was dehydrated in a graded series of alcohol treatments (15 min in alcohol 30% to 95% and 30 min in 100%). The sample was then dried using a critical point dryer for scanning electron microscopy (SEM). Finally, the sample was coated with Au-Pd alloy and examined with a scanning electron microscope. The composition of the corrosion products was analyzed with the SEM and energy dispersive x-ray analysis (EDXA).

RESULTS AND DISCUSSION

Stoichiometry of a Mixed Population SRB Biofilm on Corrosion Coupon

Stoichiometric determinations were conducted in batch conditions after biofilm had accumulated in the open channel flow reactor. The exhaustion of lactate corresponded to plateau values for sulfate reduction and sulfide production (Figure 2). The decrease in sulfide concentration was due to the continuous purging of nitrogen in the reactor. Both sulfate reduction and sulfide production agreed with the theoretical calculations based on the stoichiometry of lactate oxidation:



The stoichiometric ratios provide strong evidence that SRB dominated the biofilm under the experimental conditions.

Effect of Substrate Loading Rates on Corrosion of Mild Steel

Biofilm accumulation was strongly dependent on substrate loading rate. At constant influent substrate (lactate) concentration and at low dilution rate (0.04 h^{-1}), there was enough residence time (25 h) for the organisms to grow in the bulk liquid. This resulted in a thin biofilm. It appears that bulk liquid cells could compete effectively with biofilm cells for substrate. However, at high dilution rate (0.75 h^{-1}), there was not enough time for organisms to grow in the bulk liquid and a thick biofilm accumulated. The formation of iron sulfide precipitates on the mild steel surface was purposefully prevented before the biofilm accumulation to reduce the interference of iron sulfide with the cathodic depolarization reaction. Dissolved sulfide in the bulk liquid and hydrogen sulfide in the gas phase were flushed away after some initial biofilm

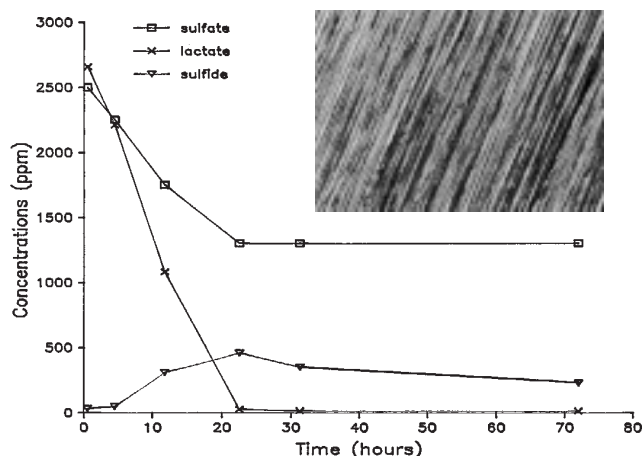
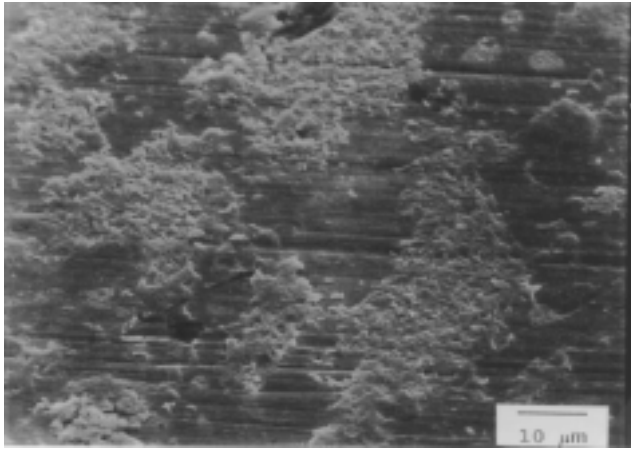


FIGURE 2. Sulfide production, lactate consumption, and sulfate degradation in mixed culture containing SRB. Attached picture ($\times 50$) indicates no iron sulfide corrosion products at the end of experiment.

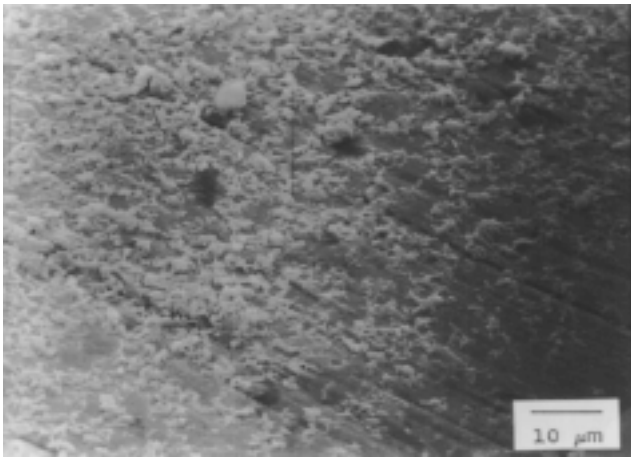
had accumulated in the open channel flow reactor. Then, corrosion experiments were initiated by insertion of clean metal coupons into the reactor followed by normal substrate input. The continuous flow experiments were conducted for 21 days.

Biofilm accumulation was a function of substrate loading rate (Figures 3 and 4), which was manipulated by changing influent flow rate (not influent substrate concentration). Biofilm thickness after 21 days reached approximately $1,000 \mu\text{m}$ at the high substrate loading rate while accumulating to approximately $5 \mu\text{m}$ at the low substrate loading rate. At the high loading rate, the biofilm was mainly composed of cells with a small amount of extracellular polymeric substances (EPS) (Figure 5). Chemical analysis of the bulk water showed similar sulfide concentration, acetate concentration, and redox potential for the two loading rates. However, there was residual lactate in the high substrate loading rate experiment even after 21 days (Tables 1 and 2). At the low substrate loading rate, the ratio of SRB in the biofilm to that in bulk water was approximately 0.1. However at high substrate loading rate, the ratio of SRB in the biofilm to that in bulk water was greater than 100 (Figure 6 and 7), which indicate that the increased substrate loading rate (i.e., higher dilution rate) creates an environment more suitable for SRB biofilm accumulation.

Specific SRB activity in bulk water or within biofilm can be monitored indirectly by specific substrate removal rate (substrate removed per cell per unit time) or specific product formation rate (product produced per cell per unit time). The specific substrate removal rate for lactate is not a good indicator of SRB activity in a mixed culture experiment since GAB may also be removing lactate. The specific sulfide formation rate is not a good indicator of SRB activity due to its volatile



(a)

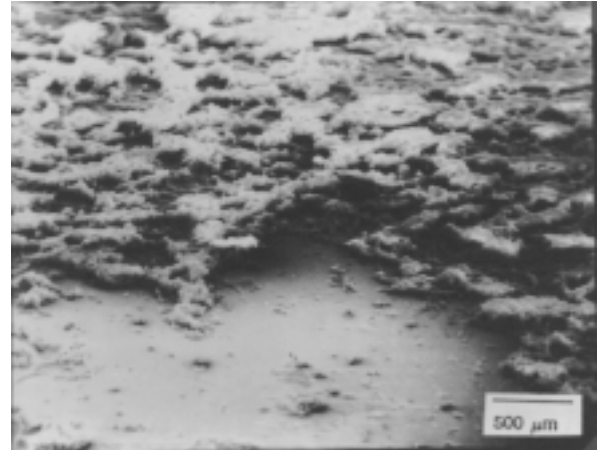


(b)

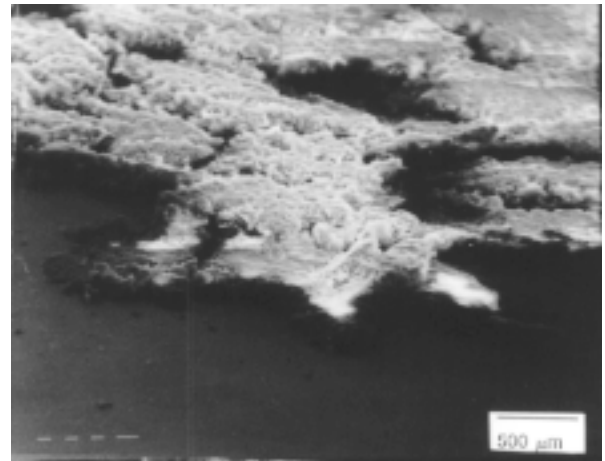


(c)

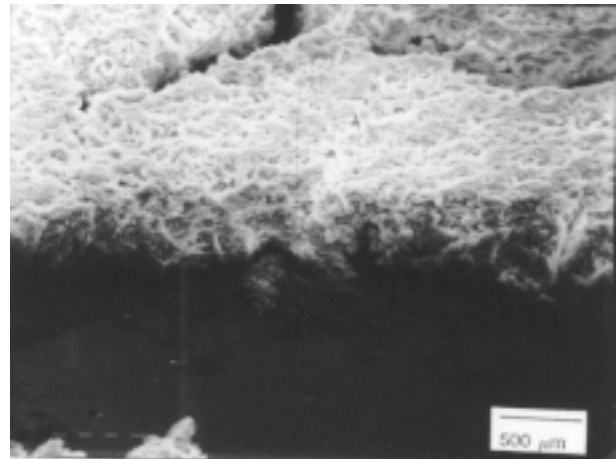
FIGURE 3. Scanning electron micrographs of biofilm grown on a mild steel surface for (a) 3 days, x 1,300, (b) 7 days, x 1,300, and (c) 21 days, x 1,300 at low substrate loading rate.



(a)



(b)



(c)

FIGURE 4. Scanning electron micrographs of biofilm accumulated on a mild steel surface for (a) 3 days, x 30, (b) 7 days, x 30, and (c) 21 days, x 30 at high substrate loading rate.

nature. However, the specific sulfate removal rate can indicate the specific SRB activity. Specific sulfate removal rate is defined as follows:

$$q_s = \frac{D(S_i - S)V}{X} \quad (2)$$

where

q_s = specific sulfate removal rate	$(M_s M_x^{-1} t^{-1})$
D = dilution rate (Q/V)	(t^{-1})
S_i = influent sulfate concentration	$(M_s L^{-3})$
S = effluent sulfate concentration	$(M_s L^{-3})$
V = working volume in the reactor	(L^3)
X = total cells in the biofilm or bulk liquid	(M_x)
Q = influent flow rate	$(L^3 t^{-1})$

The SRB activity can be obtained by following:

$$\text{SRB activity} = q_s X = D(S_i - S)V \quad (3)$$

According to Equation (3), SRB activity is 21.6 mg/h at low substrate loading rate and 338 mg/h at high substrate loading rate at 21 days. However, the increased SRB activity did not enhance the corrosion of mild steel. There was no detectable difference in weight loss due to change in loading rates and no pitting or localized corrosion observed on the metal surface under open-circuit conditions after 21 days. Metal surface analysis and electrochemical measurements provide further evidence that corrosion was insignificant. Scratch lines on the coupon were observed after 21 days under the biofilm and no iron

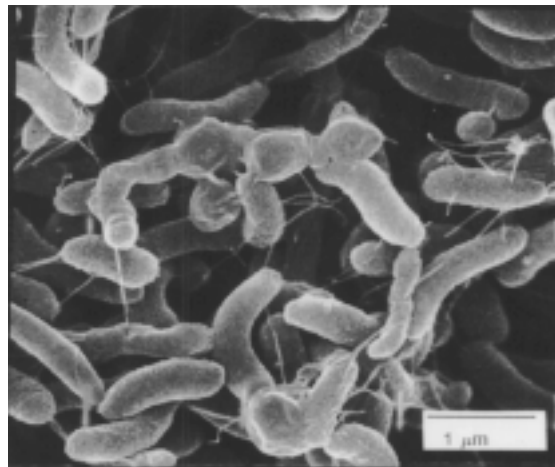


FIGURE 5. Scanning electron micrograph of a biofilm accumulated on a mild steel surface for 21 days at high substrate loading rate (x 20,000).

sulfide film formed on the coupon (Figure 8). An x-ray dot map (Figure 9) indicated no iron in the biofilm. No cathodic depolarization occurred either at low (Figure 10) or high (Figure 11) substrate loading rates in the absence of ferrous iron. At high substrate loading rate, the cathode was slightly polarized as a thick biofilm accumulated and was depolarized as the biofilm was removed (Figure 12). The difference is attributed to polarization by the thick biofilm. Presumably, a diffusion barrier formed between the bulk water and the metal surface as a thick biofilm accumulated. The diffusion barrier prevented the diffusion of OH^- or H_2 (cathodic reaction products) away from the metal

TABLE 1

Sulfate and Lactate Consumption and Sulfide and Acetate Production in Bulk Water Containing Mixed Culture Anaerobic Bacteria and SRB at Low Substrate Loading Rate

Chemicals Time	Sulfate Consumed	Lactate Consumed	Sulfide Produced	Acetate Produced	Redox Potential
3 days	125 ppm	182 ppm	—	—	-0.495 V
7 days	115 ppm	202 ppm	—	—	—
21 days	120 ppm	230 ppm	58 ppm	50 ppm	-0.465 V

TABLE 2

Sulfate and Lactate Consumption and Sulfide and Acetate Production in Bulk Water Containing Mixed Culture Anaerobic Bacteria and SRB at High Substrate Loading Rate

Chemicals Time	Sulfate Consumed	Lactate Consumed	Sulfide Produced	Acetate Produced	Redox Potential
3 days	90 ppm	110 ppm	46 ppm	40 ppm	-0.440 V
7 days	120 ppm	120 ppm	46 ppm	43 ppm	-0.420 V
21 days	100 ppm	127 ppm	47 ppm	41 ppm	-0.483 V

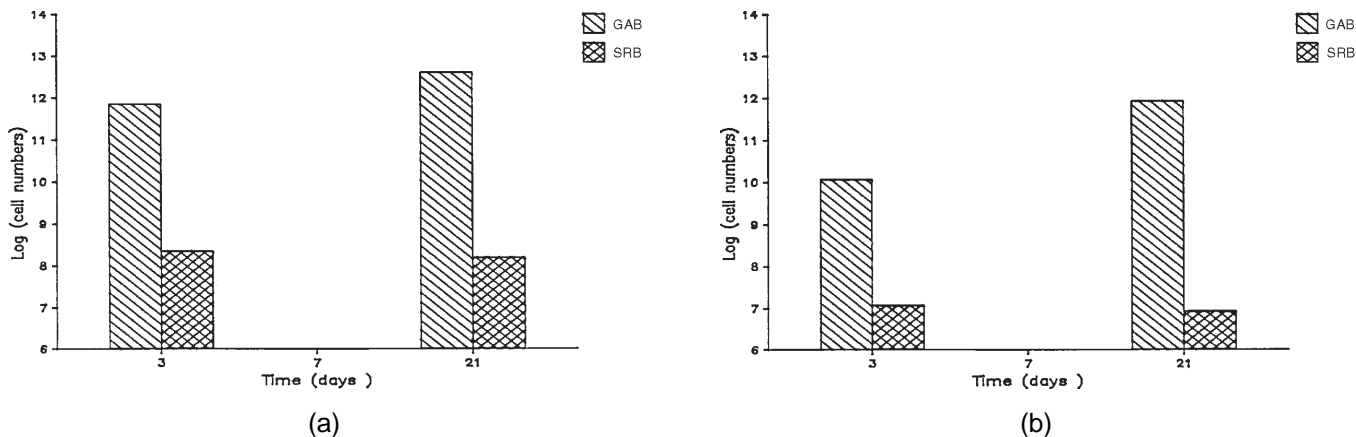


FIGURE 6. MPN for GAB and SRB at (a) low substrate loading rate and (b) high substrate loading rate in the bulk water at different exposure times (cell numbers represent the total cell numbers).

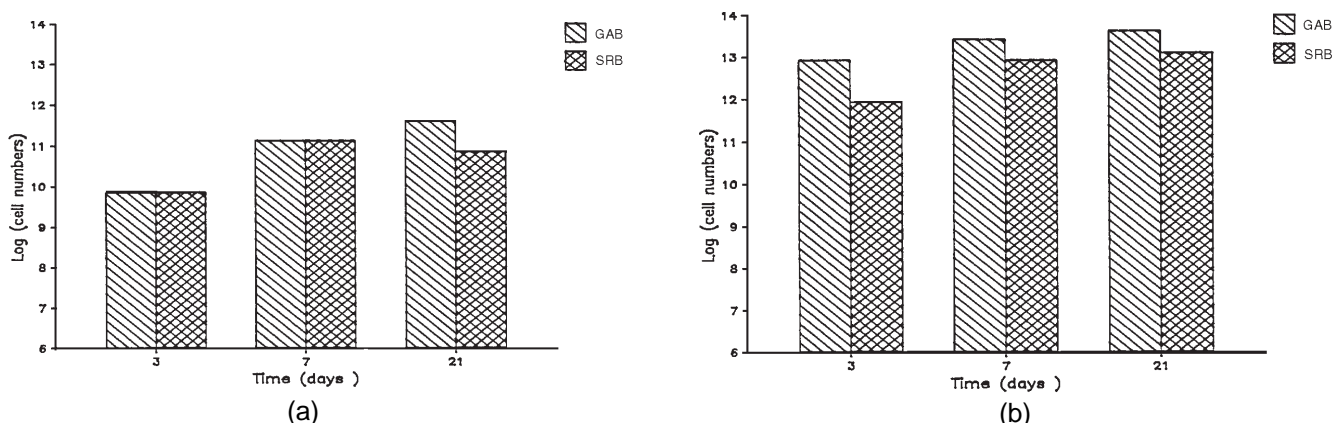


FIGURE 7. MPN for GAB and SRB at (a) low substrate loading rate and (b) high substrate loading rate in the biofilm at different exposure times (cell numbers represent the total cell numbers).

surface during polarization and reduced cathodic current density.¹⁴ The same result was observed when a coupon was coated with a similar thickness of 1.5% agar instead of a SRB biofilm (Figure 13).

In a batch culture experiment, Salvarezza and Videla¹⁵ used potentiostatic polarization techniques to show that SRB influence the metal in a similar manner to nonbiogenic sulfide, which shifts the pitting potential to a more active value. The pitting potential is defined as the potential where current increases dramatically. The pitting potential becomes more noble as the biofilm becomes thicker both at low (Figure 14) and high (Figure 15) substrate loading rates. This indicates that the pitting tendency of mild steel becomes more difficult with time. Pits were detected on the metal surface after anodic polarization at both substrate loading rates (Figure 16).

The probable role of biofilms in the protection of metal against corrosion in SRB environments has been proposed by Gaylarde and Videla.¹⁶ This investigation suggests that the biofilms possibly

increase the activation energy for hydrogen reduction and/or recombination on the steel surface.

Corrosion of Mild Steel on Precoated Iron Sulfide Film Followed by Biofilm Accumulation

The steel surface was precoated with a layer of iron sulfide film followed by biofilm accumulation at the high substrate loading rate. The precoating procedure consisted of flushing the mild steel coupons with 30 mg/L sulfide solution under anaerobic, abiotic conditions at pH 8 for one day.

Localized corrosion under open-circuit conditions was observed when biofilm developed on a precoated coupon. The pitting potential shifted to a more active value (150 mV, [Figure 17]), which is consistent with observation after the biofilm and iron sulfide film was removed. There was little change in cathodic polarization curves as the experiment proceeded (Figure 18). Microscopic examination revealed intergranular attack at inclusions (Al, Mn, and Fe) and

grain boundary triple points found in the localized corrosion area (Figure 19). Aggregates of bacteria and iron sulfide crystals (confirmed by EDAX) were found in the localized corrosion area underneath the iron sulfide film and biofilm (Figure 20). The accumulation of bacteria within the localized corrosion area may accelerate corrosion by enhancing the cathodic depolarization within the area and may lead to incipient open pits or through-wall corrosion, which is commonly found in industry and supposedly due to microbial processes.

In general, biofilm accumulation appears to reduce the spalling of iron sulfide film as compared to the abiotic conditions under similar chemical environments.¹⁷ However, the risk of localized corrosion is significant. Initiation of the localized corrosion process is believed to be strongly related to metallurgical heterogeneities in the metal alloy matrix. Following the initiation of localized corrosion, the attack may be propagated if there are active SRB within the localized corrosion area.

Effect of Ferrous Ion on Corrosion of Mild Steel with a Precoated Biofilm

Mild steel coupons were precoated with biofilm at a high substrate loading rate for one week in the

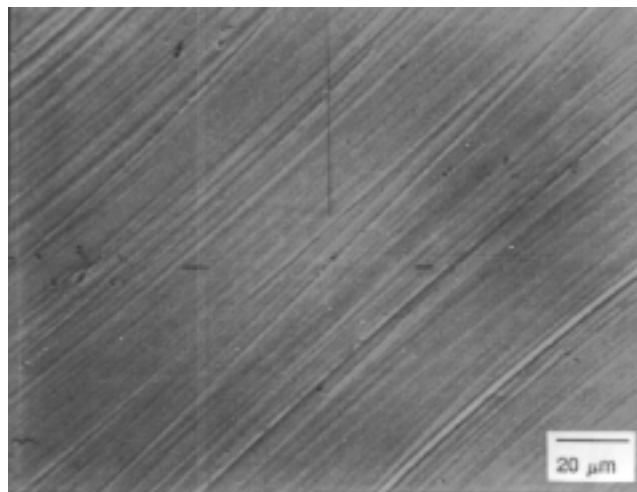


FIGURE 8. Scanning electron micrograph of a mild steel surface after biofilm has been removed at 21 days (x 700).

absence of ferrous ions followed by weekly step increases in ferrous ion to 1, 10, 60 mg/L.

The accumulation of iron sulfide in the biofilm at different ferrous ion concentrations is illustrated in Figure 21. Very little corrosion occurred at zero or low ferrous ion concentrations (0, 1, and 10 mg/L), but

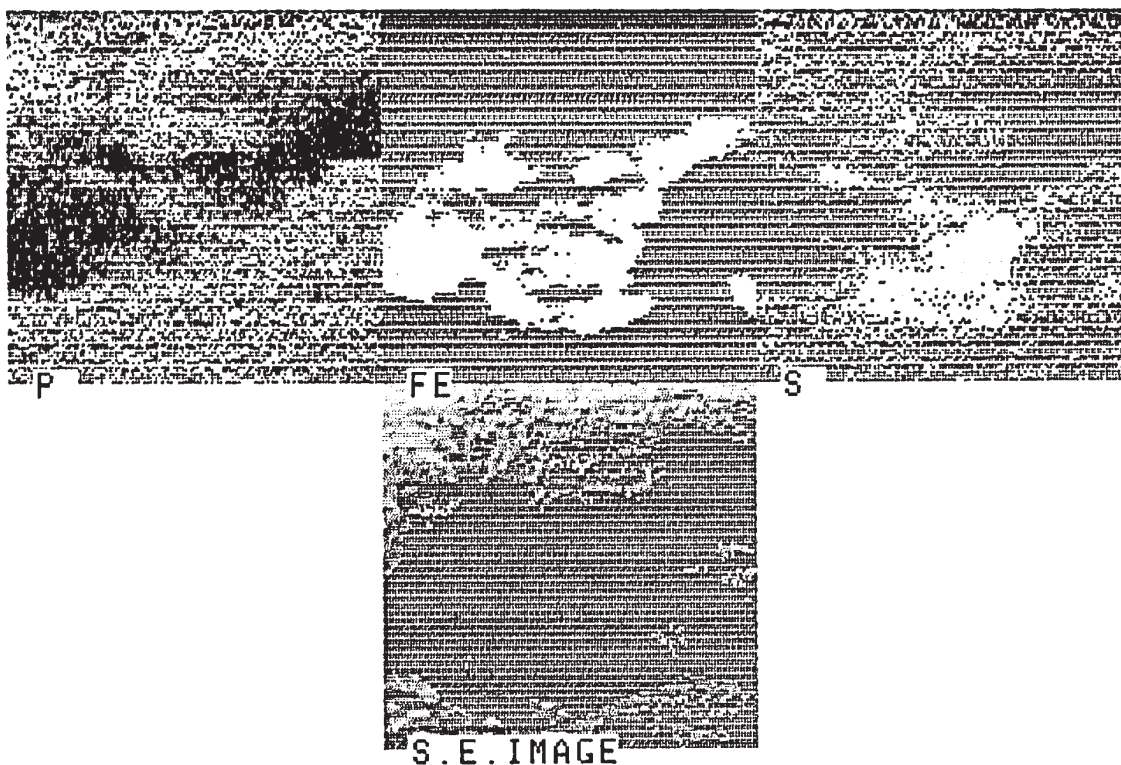


FIGURE 9. X-ray dot map indicating the elemental distribution of iron, sulfur, and phosphorous on the top of biofilm and the cross section of biofilm and metal surface.

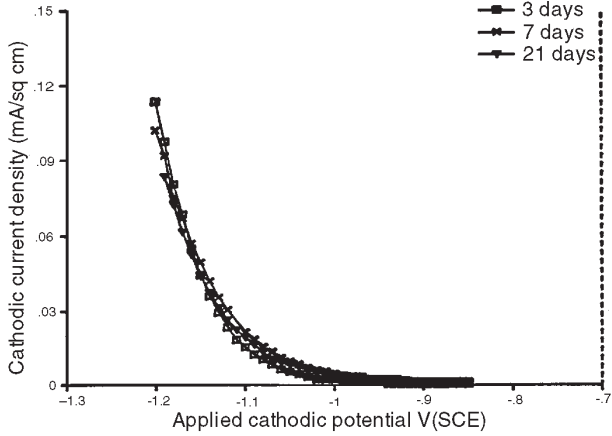


FIGURE 10. Cathodic polarization curves of mild steel at low substrate loading rate at different exposure times.

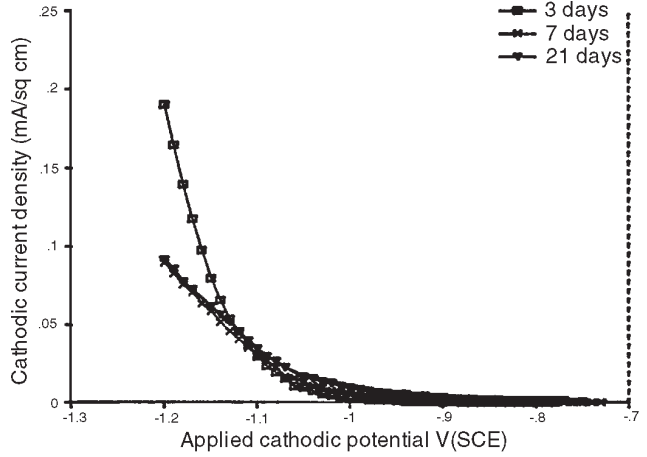


FIGURE 11. Cathodic polarization curves of mild steel at high substrate loading rate at different exposure times.

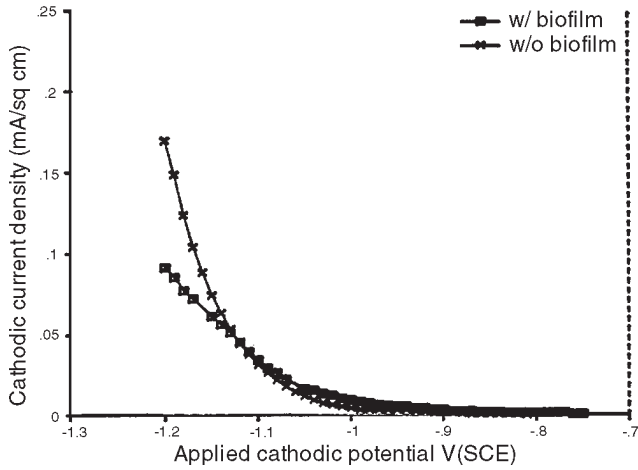


FIGURE 12. Cathodic polarization curves of mild steel before and after biofilm has been removed at high substrate loading rate.

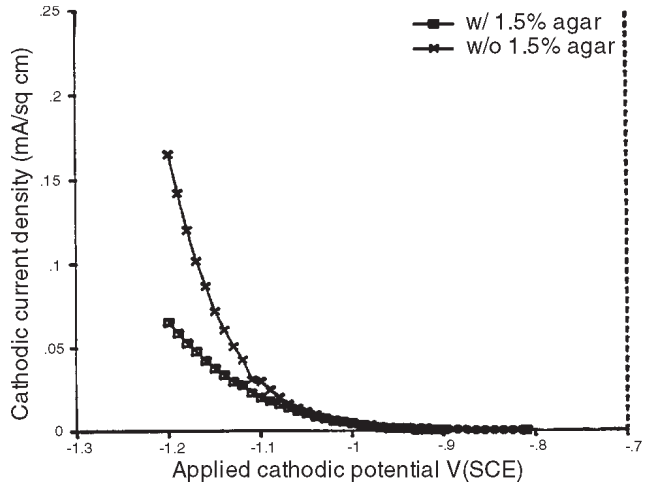


FIGURE 13. Cathodic polarization curves of mild steel before and after coupon is coated with 1.5% agar.

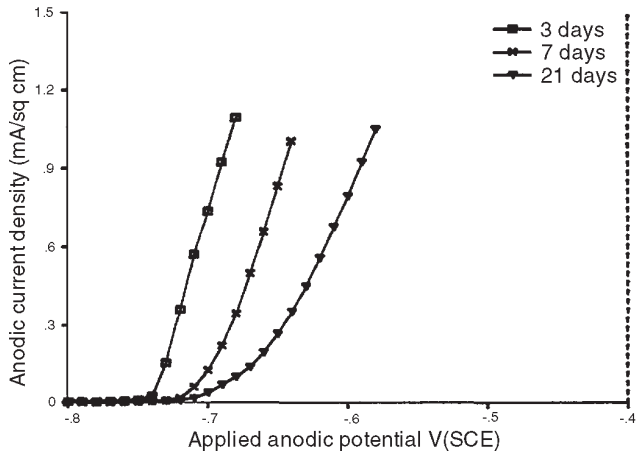


FIGURE 14. Anodic polarization curves of mild steel at low substrate loading rate at different exposure times.

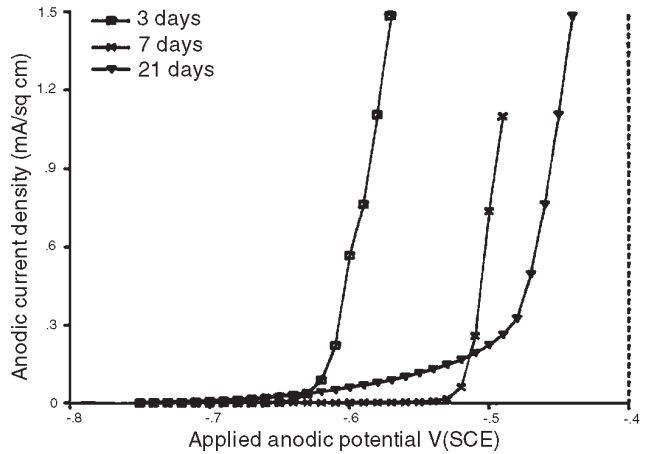


FIGURE 15. Anodic polarization curves of mild steel at high substrate loading rate at different exposure times.

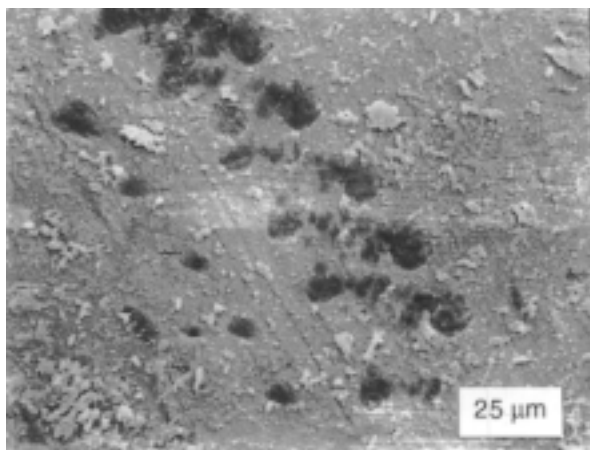


FIGURE 16. Scanning electron micrograph of a mild steel surface indicating pitting attack after anodic polarization ($\times 750$).

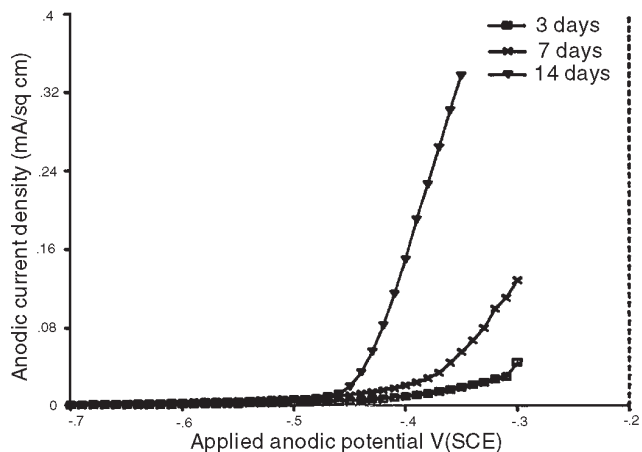


FIGURE 17. Anodic polarization curves of mild steel on a precoated iron sulfide film followed by biofilm accumulation at different exposure times.

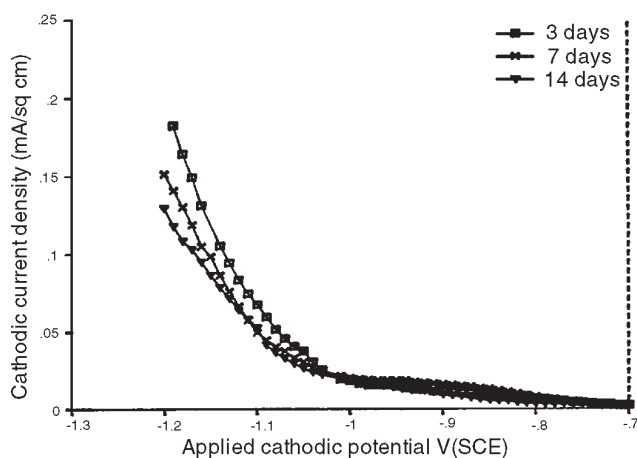


FIGURE 18. Cathodic polarization curves of mild steel on a precoated iron sulfide film followed by biofilm accumulation at different exposure times.

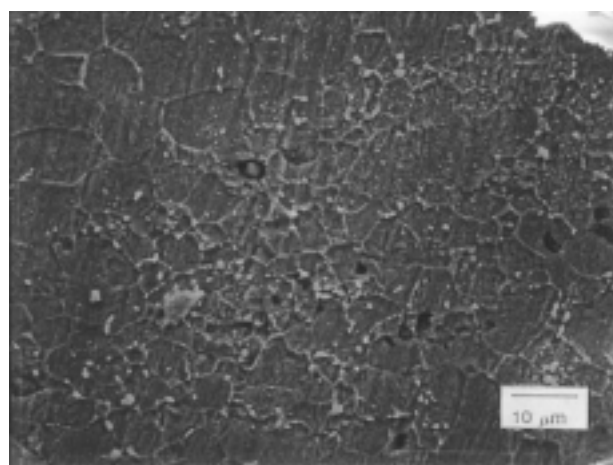
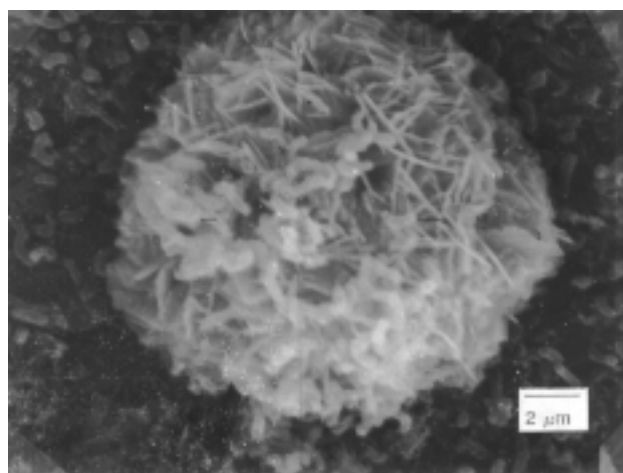
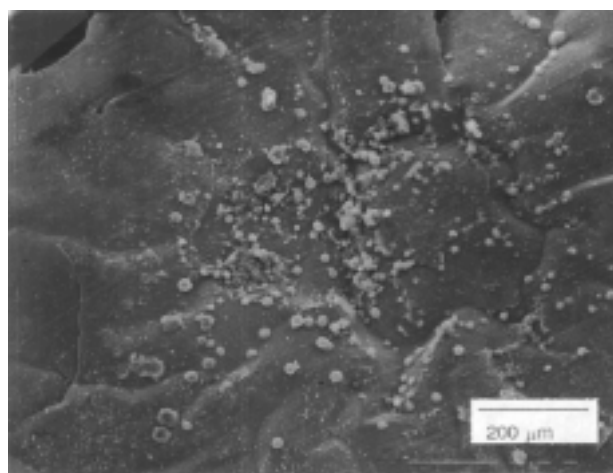


FIGURE 19. Scanning electron micrograph of a mild steel surface indicating intergranular attack in the localized corrosion area; inclusions (Al, Mn, and Fe) and grain boundary triple points were found in this area ($\times 1,200$).

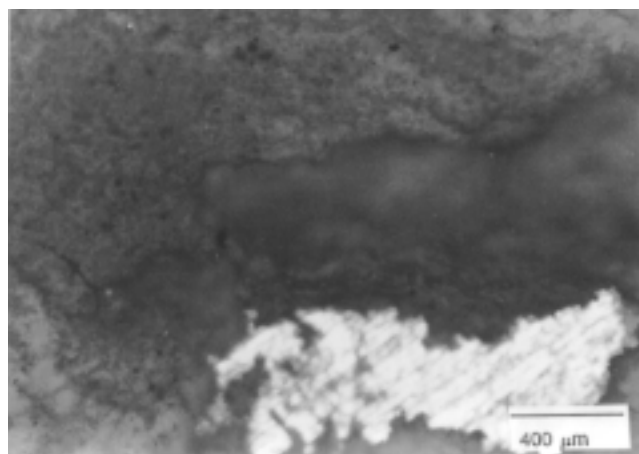


(a)

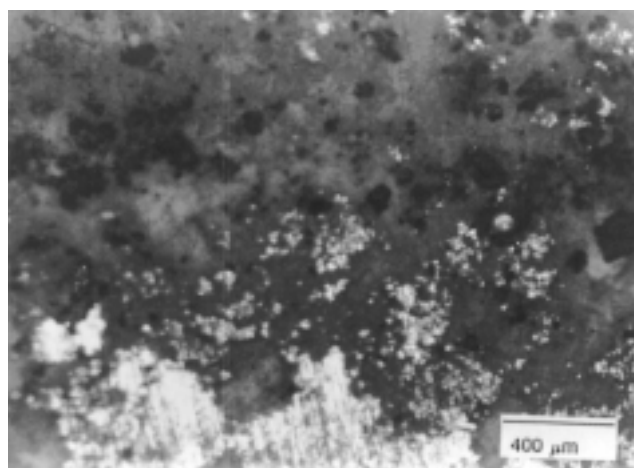


(b)

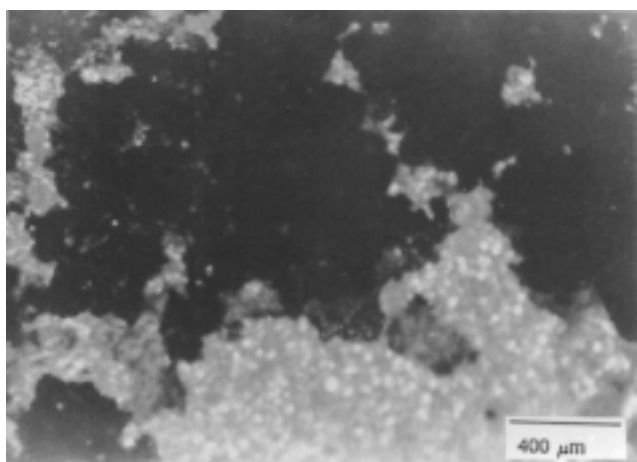
FIGURE 20. (a) Accumulation of bacteria and iron sulfide crystals in the localized corrosion area ($\times 100$). (b) Detached iron sulfide film above localized corrosion area ($\times 5,300$).



(a)



(b)



(c)

FIGURE 21. Accumulation of iron sulfide on a precoated biofilm at different ferrous ion concentrations. (a) 1 mg/L, x 50, (b) 10 mg/L, x 50, and (c) 60 mg/L, x 50.

accumulation of iron sulfide particles increased in the biofilm. There was no direct contact between iron sulfide particles and the mild steel surface. However, iron-rich media (60 mg/L) resulted in the precipitation of all the biogenic sulfide (Figure 22). An x-ray dot map indicates that the iron sulfide particles penetrate through the biofilm and contact the metal surface (Figure 23). Cathodic and anodic currents increased dramatically as ferrous ions increased from 10 to 60 mg/L (Figures 24 and 25).

AC impedance measurements cannot accurately detect localized corrosion. However, AC impedance can assess the rate of generalized corrosion. Nyquist plots indicated that the charge transfer resistance (R_{ct} , the diameter of the semicircle, which is inversely proportional to the corrosion rate) decreased dramatically as ferrous ion concentration increased from 10 to 60 mg/L (Figure 26). There was no protective coating of iron sulfide film formed under the biofilm in the iron-rich media. Intergranular attack was observed over the entire metal surface after precipitated iron sulfide and biofilm was removed (Figure 27). Thus, corrosion of mild steel was enhanced by the accumulated iron sulfide due to cathodic and anodic depolarization.

In the anaerobic biofilms containing SRB, corrosion rate can be accelerated through two mechanisms: (1) corrosion rate is accelerated by cathodic depolarization but is limited by diffusion of hydrogen sulfide through the corrosion product layer (concentration polarization), as observed under abiotic conditions.¹⁸ (2) Corrosion rate is accelerated by cathodic depolarization but is not limited by concentration polarization. In this case, accumulation of sessile SRB in the loose iron sulfide accelerates corrosion presumably by reducing the diffusion distance for the biogenic sulfide to reach the metal surface.

Gaylarde and Johnson¹⁹ report that biofilm (sessile) SRB on the metal surface results in a higher corrosion rate as compared to the corrosion rate due to planktonic bacteria alone. These observations support the second mechanism. However, the corrosion rate may be reduced when sulfate or lactate diffusion within the biofilm limits the rate of microbial activity.

The loose iron sulfide particles apparently play a more important role than the bacteria in the anaerobic corrosion process under the conditions of the reported experiments. The iron sulfide particles are cathodic to the mild steel but do not act as permanent cathodes unless dissolved sulfide or SRB (which produce dissolved sulfide) are present. The role of the mixed SRB biofilm on the anaerobic corrosion of mild steel is to continuously supply hydrogen sulfide to keep loose iron sulfide particles cathodically active. This

interpretation of the experimental results is consistent with proposals by Miller.²⁰

SUMMARY/CONCLUSIONS

The experimental investigations reported herein provide strong evidence that corrosion of mild steel was insignificant even in the presence of an active SRB biofilm. This may be attributed to the high activation energy for hydrogen reduction and/or recombination. However, in the combined presence of an SRB biofilm with dissolved oxygen, dissolved iron, and iron sulfide, corrosion is enhanced. Hardy and Bown²¹ demonstrated that high corrosion rates and severe pitting attack on mild steel, sometimes observed in the field, occurs when oxygen is introduced into the system. Under completely anaerobic conditions, iron sulfide may play a similar key role in the corrosion process. The physical forms of iron sulfide determined the type of corrosion (e.g., localized corrosion vs uniformly corrosion) in the presence of SRB biofilm. Generalized attack was observed where there was loose iron sulfide precipitation under the SRB biofilm, while localized attack was observed at the defect sites of protective iron sulfide film.

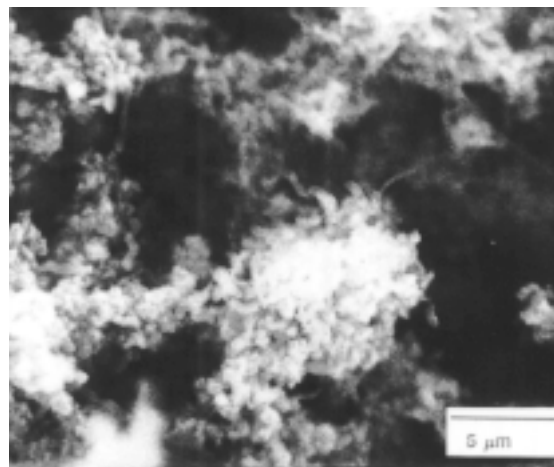


FIGURE 22. Scanning electron micrograph of biofilm when the media contain 60 mg/L ferrous ion concentration ($\times 4,000$).

- ❖ The combination of biofilm process analysis with electrochemical measurements and surface analysis offers a useful tool for investigating microbial corrosion problems.
- ❖ Corrosion cannot be initiated by SRB on mild steel in the absence of ferrous ion, regardless of dilution rate.

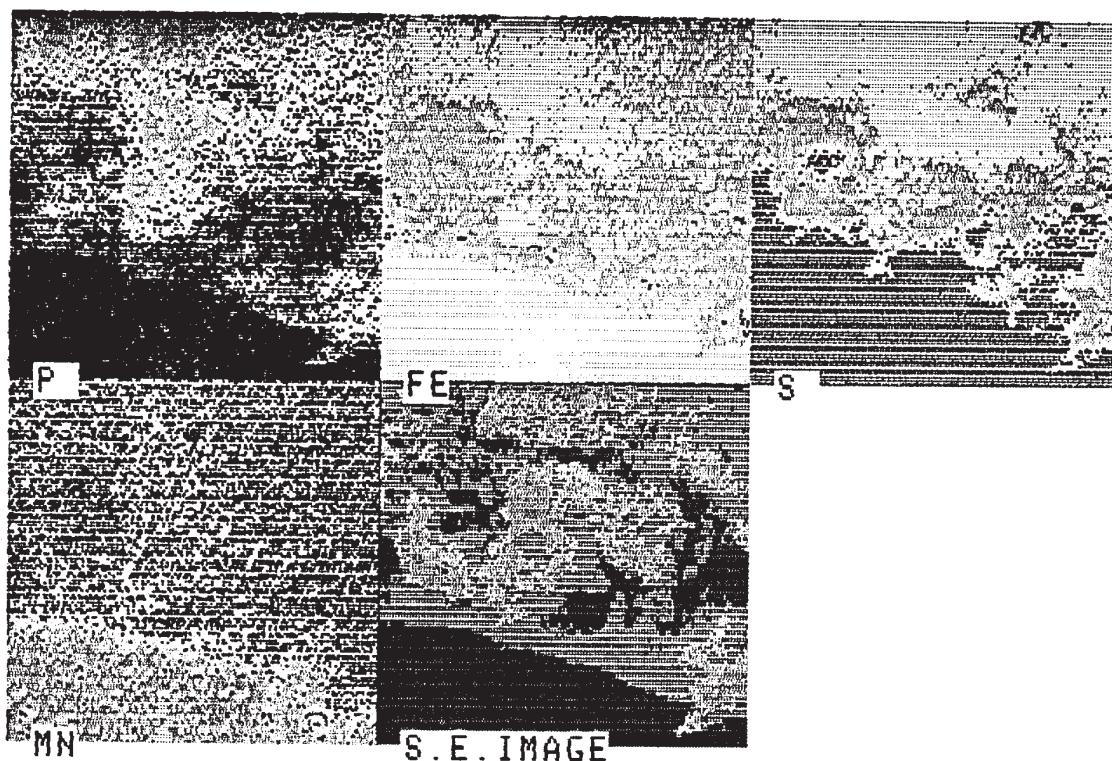


FIGURE 23. X-ray dot map indicating the elemental distribution of iron, sulfur, and phosphorus on the top and cross section of biofilm and metal substratum.

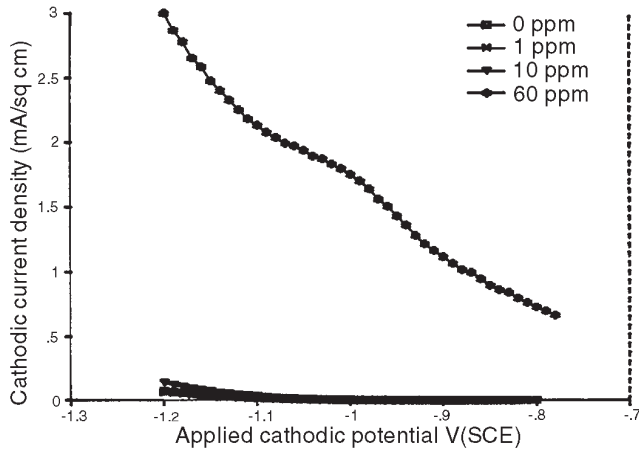


FIGURE 24. Cathodic polarization curves of mild steel on a pre-coated biofilm followed by step increase in ferrous ion concentrations.

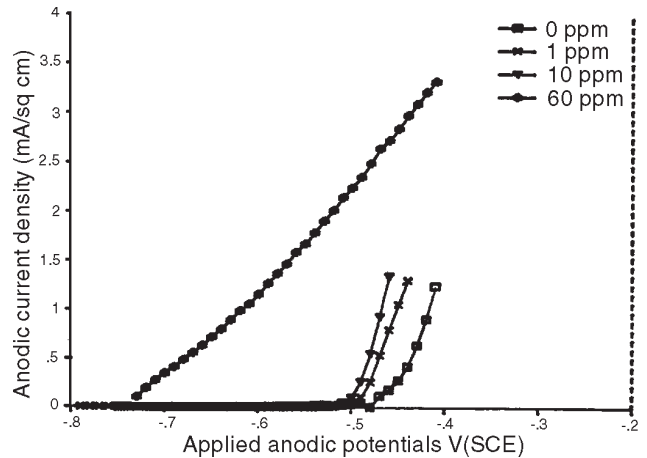


FIGURE 25. Anodic polarization curves of mild steel on a pre-coated biofilm followed by step increase in ferrous ion concentrations.

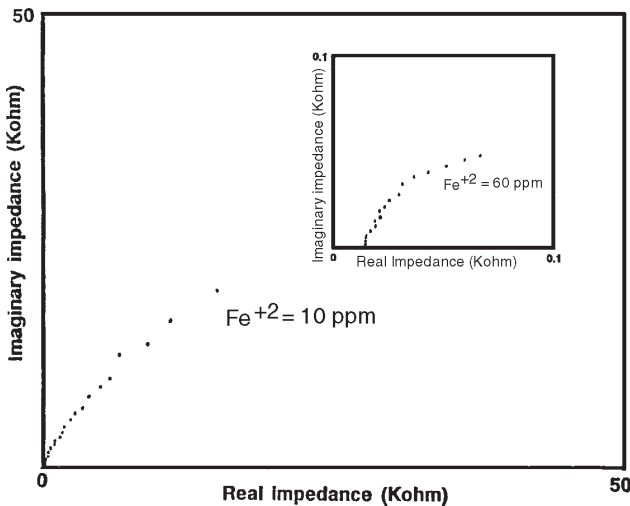


FIGURE 26. Nyquist plots for mild steel on a pre-coated biofilm at different ferrous ion concentrations.

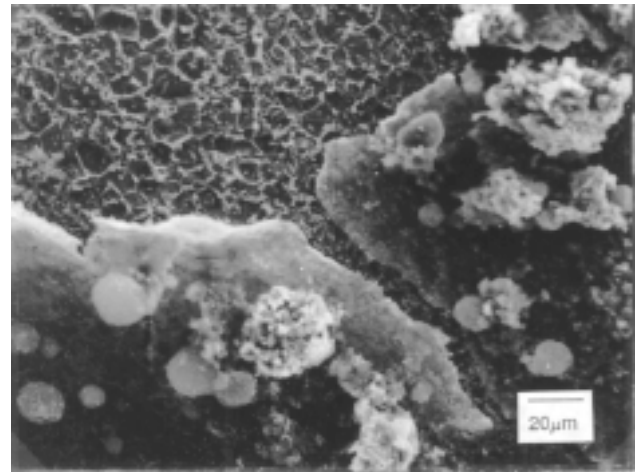


FIGURE 27. Scanning electron micrograph of a mild steel surface indicating the nonprotective iron sulfide film and intergranular attack over the entire metal surface (x 550).

- ❖ There is no cathodic depolarization and no correlation between corrosion and SRB activity in the absence of ferrous ion in a biofilm reactor at pH = 8.
- ❖ Accumulation of bacteria on a pre-coated iron sulfide film reduces the possibility of spalling of sulfide film but does not eliminate the potential for localized corrosion.
- ❖ Corrosion of mild steel in the presence of biofilm will be enhanced by suspended iron sulfide once the iron sulfide particle contacts the metal surface
- ❖ Intergranular attack is always associated with loose iron sulfide deposition.

ACKNOWLEDGMENTS

The authors acknowledge partial support from the National Science Foundation project no. CTB-

8420785, "An Investigation of Mechanisms for Microbially Assisted Corrosion," and the NSF Center for Interfacial Microbial Process Engineering. The authors thank V. Griffiths, Montana College of Mineral Science and Technology, for making SEM/EDAX instrumentation available. A. Camper and D. Davies are acknowledged for their valuable suggestions. The IPA Industrial Associates are acknowledged for their support of this work.

REFERENCES

1. P.F. Sanders, W.A. Hamilton, Proceedings of the International Conference on Biologically Induced Corrosion (Houston, TX: NACE, 1985), p. 47.
2. J.S. Smith, J.D.A. Miller, Brit. Corros. J. 10 (1975): p. 136.
3. G.H. Booth, L. Elford, D.S. Warkerley, Brit. Corros. J. 3 (1988): p. 242.
4. G.H. Booth, P. M. Cooper, D. S. Wakerley, Brit. Corros. J. 1 (1988): p. 345.

5. G.H. Booth, J.A. Robb, D.S. Wakerley, 3rd Int. Congress on Metallic Corrosion, Moscow, 2 (1967), p. 542.
6. R.L. Starkey, Proceedings of the International Conference on Biologically Induced Corrosion (Houston, TX: NACE, 1985), p. 3.
7. V.W. Kühn, van der Vlugt, Water 18 (1934): p. 147.
8. R.H. King, J.D.A. Miller, J.S. Smith, Brit. Corros. J. 8 (1973): p. 137.
9. J.A. Costello, South African Journal of Science 70 (1974): p. 202.
10. W.A. Hamilton, S. Maxwell, Proceedings of the International Conference on Biologically Induced Corrosion (Houston, TX: NACE, 1985), p. 131.
11. P.H. Nielsen, Appl. Environ. Microbiol. 53 (1987): p. 27.
12. Standard Methods for the Examination of Water and Waste Water, 13th ed. (Washington, D.C.: American Public Health Association, 1971).
13. J.D. Cline, Limnol Oceanogr 14 (1969): p. 454.
14. Z. Lewandowski, W.C. Lee, W.G. Characklis, B.J. Little, Corrosion 45 (1989): p. 92.
15. R.C. Salvarezza, H.A. Videla, Corrosion 36 (1980): p. 550.
16. C.C. Gaylarde, H.A. Videla, International Biodeterioration 23 (1987): p. 91.
17. W.C. Lee, W.G. Characklis, 8th International Symposium on Biodeterioration and Biodegradation, Windsor, Canada (Essex, United Kingdom: Elsevier, 1991), p. 89.
18. R.L. Martin, R.R. Annand, Corrosion 36 (1981): p. 297.
19. C.C. Gaylarde, J.M. Johnson, Microbial Adhesion to Surface, Berkeley, R.C.W. Lynch, J.W., P.R. Rutter, B. Vincent, eds. (Chichester, United Kingdom: Ellis Harwood Ltd., 1980), p. 511.
20. J.D.A. Miller, Metals, Microbial Biodeterioration, A.H. Rose, ed. (New York, NY: Academic Press, 1981), p. 149.
21. J.A. Hardy, J.L. Bown, Corrosion 40 (1984): p. 650.